Published in final edited form as:
J Biol Chem. 2002 November 22; 277(47): 45537–45546.

Dual-substrate Specificity Short Chain Retinol Dehydrogenases from the Vertebrate Retina[*,S]

Françoise Haeseleer[‡,§], **Geeng-Fu Jang**[‡,§], **Yoshikazu Imanishi**[‡,§], **Carola A. G. G. Driessen**[¶], **Masazumi Matsumura**[‖], **Peter S. Nelson**[‖], and **Krzysztof Palczewski**[‡,**,‡‡,§§]

‡*From the Department of Ophthalmology, University of Washington, Seattle, Washington 98195*

******From the Department of Pharmacology, University of Washington, Seattle, Washington 98195*

‡‡*From the Department of Chemistry, University of Washington, Seattle, Washington 98195*

¶*Department of Biochemistry, University of Nijmegen, 6500 HB Nijmegen, The Netherlands*

‖*The Division of Human Biology, Fred Hutchinson Cancer Research Center, Seattle, Washington 98109*

Abstract

Retinoids are chromophores involved in vision, transcriptional regulation, and cellular differentiation. Members of the short chain alcohol dehydrogenase/reductase superfamily catalyze the transformation of retinol to retinal. Here, we describe the identification and properties of three enzymes from a novel subfamily of four retinol dehydrogenases (RDH11–14) that display dual-substrate specificity, uniquely metabolizing all-*trans*- and *cis*-retinols with C_{15} pro-*R* specificity. RDH11–14 could be involved in the first step of all-*trans*-and 9-*cis*-retinoic acid production in many tissues. RDH11–14 fill the gap in our understanding of 11-*cis*-retinal and all-*trans*-retinal transformations in photoreceptor (RDH12) and retinal pigment epithelial cells (RDH11). The dual-substrate specificity of RDH11 explains the minor phenotype associated with mutations in 11-*cis*-retinol dehydrogenase (*RDH5*) causing fundus albipunctatus in humans and engineered mice lacking *RDH5*. Furthermore, photoreceptor RDH12 could be involved in the production of 11-*cis*-retinal from 11-*cis*-retinol during regeneration of the cone visual pigments. These newly identified enzymes add new elements to important retinoid metabolic pathways that have not been explained by previous genetic and biochemical studies.

Retinoids are indispensable light-sensitive elements of vision and also serve as essential modulators of cellular differentiation and proliferation in diverse cell types, including those comprising the epithelium and immune system. Retinoids modulate the growth of both normal and malignant cells through their binding to retinoid receptors. All-*trans*-retinoic acid signals through specific interactions with the nuclear retinoic acid receptors, whereas its isomer, 9-*cis*-retinoic acid, is a high affinity ligand of retinoic acid receptors and retinoid X receptors. In the retina, light-dependent photoisomerization of 11-*cis*-retinylidene to the all-*trans*-retinylidene moiety of rod and cone photoreceptors is a key reaction that triggers visual

[*]This research was supported by National Institutes of Health Grants EY08061, CA75173, and DK59125, a grant from Research to Prevent Blindness, Inc. (to the Department of Ophthalmology, University of Washington), and by the E. K. Bishop Foundation. The costs of publication of this article were defrayed in part by the payment of page charges. This article must therefore be hereby marked "*advertisement*" in accordance with 18 U.S.C. Section 1734 solely to indicate this fact.

[S]The on-line version of this article (available at http://www.jbc.org) contains Supplemental Figs. 1 and 2 and Tables 1–3.

[§]These authors contributed equally to this work.
[§§]Recipient of a Research to Prevent Blindness Senior Investigator Award. To whom correspondence should be addressed: Dept. of Ophthalmology, University of Washington, Seattle, WA 98195. Tel.: 206-543-9074; Fax: 206-221-6784; E-mail: palczews@u.washington.edu.

sensation (1). Restoration of the visual chromophore occurs through a complex set of reactions, termed the retinoid cycle, in photoreceptor cells and adjacent retinal pigment epithelial cells (RPE)[1] (2). Dietary deficiencies in retinoids and retinoid precursors cause visual impairment, developmental abnormalities, and immune deficiency (3,4).

Transformations of retinoids occur mostly through enzymatic or photochemical reactions, although they readily isomerize non-enzymatically to thermodynamic equilibrium when unprotected by the retinoid-binding proteins (5). The key enzymes involved in retinoid metabolisms are alcohol and aldehyde dehydrogenases that convert retinols to aldehydes and aldehydes to carboxylic acids, respectively. The first oxidation reaction is catalyzed by a large number of enzymes from the SDR superfamily (6,7) and by classic medium chain alcohol dehydrogenases (8). SDRs are weakly conserved in their primary sequences, with the exception of key residues involved in catalysis, nucleotide recognition, and members of closely related subfamilies. SDRs also display NADP or NAD cofactor preference and, if they are retinol dehydrogenases (RDHs), favor all-*trans*- or *cis*-retinol substrates. Some RDH enzymes also catalyze the oxidation of steroids in addition to retinols (9). Localized expression of these enzymes in the photoreceptor and RPE cells, where heavy traffic of diffusible retinoids occurs, strongly suggest that retinols and retinals are their *in vivo* substrates. The role of specific SDRs in vision has been determined from the biochemical characterization of enzymes isolated from specific compartments of the retina, analyses of retinoid flow in genetically engineered mice, and from associations of human visual dysfunctions with specific disabling mutations in one of the SDR genes, *RDH5* (for review, see Ref. 2).

The present study was undertaken to resolve the discrepancy between biochemical and genetic analyses of the RDH activity responsible for 11-*cis*-retinal and 9-*cis*-retinal production. An enzyme encoded by the *RDH5* gene (10,11), 11-*cis*-RDH, was proposed to be responsible for both 11-*cis*-retinal and 9-*cis*-retinal production due to its relaxed substrate specificity (12-15). However, the disruption of this gene in a mouse model led to uninterrupted production of 11-*cis*-retinal (16,17) and a lack of any embryonic abnormalities. Furthermore, patients with fundus albipunctatus who also have a disabling mutation in the *RDH5* gene still show efficient production of the chromophore, albeit with slower kinetics (18,19). Here, we characterized members of a novel subfamily of SDRs cloned from the retina that display novel properties of dual *cis*- and all-*trans*-retinol substrate specificities. The recognition of both types of isomers studied by stereospecific substrates unravels a novel mode of substrate recognition. The RDH11 transcript has been previously identified as one that exhibits increased expression on exposure to androgens in the LNCaP prostate cancer cell line (20) and is proposed to be involved in the metabolism of retinoids (21).

MATERIALS AND METHODS

Cloning of Human RDH11–14—Full-length RDHs were amplified by PCR from human (RDH11–13) or mouse (RDH14) retina cDNA libraries using primers FH497 (5′-GAGATGGTTGAGCTCATGTTC-3′) and FH498 (5′-GTTAGTCTATTGGGAGGCC3-′) for RDH11, FH500 (5′-acgatgctggtcaccttgggactg-3′) and FH501 (5′-ACGATGCTGGTCACCTTGGGACTG-3′) for RDH12, FH502 (5′-ATGAGCCGCTACCTGCTGCCG-3′) and FH503 (5′-TTATCTGGGGAGGGGCTGCTC-3′) for RDH13, and FH490 (5′-GTTATGGCAGTGGCTAGTGTGG-3′) and FH491 (5′-

[1]The abbreviations used are: RPE, retinal pigment epithelial (cells); SDR, short chain alcohol dehydrogenase/reductase; RDH, retinol dehydrogenase; prRDH, photoreceptor RDH; HPLC, high performance liquid chromatography; DTT, dithiothreitol; MES, 4-morpholineethanesulfonic acid; EST, expressed sequence tag; kb, kilobases; ROS, rod outer segments; BTP, 1,3-bis[tris(hydroxymethyl) methylamino] propane.

CTATTTTAGAATGCCAACCATCACTT-3′) for RDH14. The reactions were cycled through 35 cycles of 94 °C for 30 s and 68 °C for 2.5 min followed by 7 min at 68 °C. The PCR products were cloned in the pCRII-TOPO vector (Invitrogen) and sequenced by dideoxyterminator sequencing (ABI-Prism, PerkinElmer Life Sciences).

Expression of RDH12–14 in Escherichia coli—The coding sequences for RDH12 and RDH14 were cloned as a fragment into *Bam*HI-*Xho*I or *Eco*RI-*Xba*I sites in pMAL-c2X (New England Biolabs). This joins RDH12 and RDH14 in fusion with the maltose-binding protein. RDH12 and RDH14 were expressed in TOP10 bacteria after induction with 0.5 mM isopropyl-1-thio-β-D-galactopyranoside and purified on an amylose column according to the manufacturer's protocol. The coding sequence for RDH13 was cloned into *Eco*RI-digested pET30A. This fusion construct joins RDH13 to a His_6 tag. RDH13 was expressed in BL21 bacteria after induction with 0.2 mM isopropyl-1-thio-β-D-galactopyranoside and purified on a Ni^{2+}-nitrilotriacetic acid column in denaturing conditions according to the manufacturer's protocol (Qiagen).

Expression of RDH11, RDH12, and RDH14 in Insect and ARPE19 Cells—The coding sequence of human RDH11, human RDH12, human RDH13, or mouse RDH14 was transferred as a *Not*I-*Kpn*I fragment in *Not*I-*Kpn*I-digested pFASTBac. Recombinant RDH baculoviruses were then obtained by transposition in DH10BAC bacteria and amplified after transfection in SF9 cells. The expression of recombinant proteins was tested 3 days after transfection, and the cells were collected for enzymatic assays. ARPE19 cells were transfected with baculoviruses, and expression was driven by the cytomegalovirus promoter as described previously (22).

Immunocytochemistry and in Situ Hybridization—The *in situ* hybridization techniques and preparation of the mouse, bovine, human and monkey retinal sections were carried out as described previously (23). cDNA fragments of mouse and human RDH12 were cloned into PCRII-TOPO vectors and linearized with appropriate endonucleases. Antisense and sense RNA probes (0.9–1 kb) were synthesized by run-off transcription from the SP6 or T7 promoter with digoxigenin-UTP, as recommended in the manufacturer's protocol (Roche Molecular Biochemicals).

For immunohistochemistry, retinal sections were blocked for nonspecific labeling by incubating in 1.5% normal goat serum in PBST buffer (136 mM NaCl, 11.4 mM sodium phosphate, 0.1% Triton X-100, pH 7.4) for 15 min at room temperature. Sections were incubated with purified anti-RDH11 monoclonal antibody or anti-RDH13 serum overnight at 4 °C. Controls were prepared by absorbing the antibodies with an excess amount of RDH11 peptide (0.5 μg/ml) or purified RDH13 (2 μg/ml). Sections were rinsed in PBST and incubated with indocarbocyanine (Cy3)-conjugated goat anti-mouse IgG. Sections were then rinsed in PBST and mounted in 50 μl of 2% 1,4-diazabicyclo-2,2,2-octane in 90% glycerol to slow photobleaching. Sections were analyzed under a confocal microscope (Zeiss LSM510). Bright field images were captured with Nomarski optics (NIKON).

Preparation of Anti-RDH11, -RDH13, -RDH14, and -RDH5—The antibody against RDH11 was generated against CHVAWVSVQARNETIAR-$CONH_2$ peptide (21). Bacterially expressed and purified RDH13 and RDH14 were used to immunize BALB/c mice to obtain anti-RDH13/14 antisera. Mouse anti-RDH5 monoclonal antibodies were raised against RDH5-His_6 purified from RDH5-His_6-infected Sf9 cells (24).

Retinoids—All reactions involving retinoids were carried out under dim-red light conditions. Retinoids were stored in *N*,*N*-dimethylformamide under argon at −80 °C. Retinoids were purified by normal phase HPLC (Beckman Instruments, Ultrasphere-Si, 4.6 mm × 250 mm) with 10% ethyl acetate, 90% hexane at a flow rate of 1.4 ml/min using an HP1100 with an on-line diode-array detector and HP Chemstation A.06.03 software.

Preparation of Proteins—Fresh bovine eyes were obtained from a local slaughterhouse (Schenk Packing Co., Inc., Stanwood, WA). ROS membranes were isolated from bovine retina using the sucrose gradient centrifugation method (25). RPE microsomes were prepared as described previously (26). Expression of RDH5 with a His_6 tag at the carboxyl terminus in Sf9 cells was reported previously (24). Horse liver alcohol dehydrogenase (Sigma/Aldrich) was purified on a Mono Q HR5/5 (Amersham Biosciences) column equilibrated with 10 mM BTP, pH 7.3, using a linear gradient from 0 to 500 mM NaCl over 60 min at a flow rate of 0.7 ml/min. The horse liver alcohol dehydrogenase fraction (eluted at 1–3 min, 0.6 mg/ml) containing the highest dehydrogenase activity when assayed with pro-*R* [4-^{3}H]NADH, and all-*trans*-retinal or 11-*cis*-retinal was used in further studies (24). L-Glutamic dehydrogenase (Sigma/Aldrich) was dialyzed against 10 mM BTP, pH 7.3, 0.1 M NaCl before use.

Preparation of Pro-R [4-^{3}H]NADH, Pro-S [4-^{3}H]NADH, Pro-R [4-^{3}H]NADPH, and Pro-S [4-^{3}H]NADPH—The preparation of pro-*R* [4-^{3}H]NADH was accomplished by utilizing the pro-*R*-specific enzyme yeast alcohol dehydrogenase (Sigma) to reduce NAD with 1-^{3}H-labeled EtOH (American Radiolabeled Chemicals, Inc.) as previously described (16). Syntheses of pro-*S* [4-^{3}H]NADH and pro-*S* [4-^{3}H]NADPH were carried out with L-glutamic dehydrogenase (Sigma), NAD(P) (Sigma), and L-[2,3-^{3}H]glutamic acid (PerkinElmer Life Sciences) as previously described (19). Synthesis of pro-*R* [4-^{3}H]NADPH was prepared with L-glutamic dehydrogenase, [4-^{3}H]NADP, and L-glutamic acid, as described previously (24). The product was purified on a Mono Q HR 5/5 column equilibrated with 10 mM BTP, pH 7.3, using a linear gradient from 0 to 500 mM NaCl over 60 min at a flow rate of 0.7–1 ml/min. Concentrations of NADH and NADPH (pH 7.4) were determined using $\varepsilon = 6{,}220$ at 340 nm, and concentrations of NAD and NADP (pH 7.4) were determined using $\varepsilon = 18{,}000$ at 260 nm (27).

Preparation of Pro-R,S-9-cis-[15-^{3}H]retinol, Pro-R,S-11-cis-[15-^{3}H]retinol, and Pro-R,S-all-trans-[15-^{3}H]Retinol and Their Corresponding 15-^{3}H-Labeled Retinals—Pro-*R,S*-9-*cis*-[15-^{3}H]retinol, pro-*R,S*-11-*cis*-[15-^{3}H]retinol, and pro-*R,S*-all-*trans*-[15-^{3}H]retinol were prepared by the reduction of their respective retinals with [^{3}H]$NaBH_4$ (PerkinElmer) as described before (24). [15-^{3}H]Retinal was synthesized by MnO_2 oxidation of the corresponding pro-*R,S*-[15-^{3}H]retinol as previously described (24).

Syntheses of Stereospecific 15-^{3}H-Labeled Retinols—Table I summarizes the syntheses of various stereospecific 15-^{3}H-labeled retinols by different dehydrogenases. pro-*R* and pro-*S* designations were used for 15-^{3}H-labeled retinols produced by the enzyme for which the stereospecificity is known (24).

Assay for RDH Activity—Activities of RDHs (recombinant Sf9 cells suspended in 20 mM BTP, pH 7.4, 0.25 mM *n*-dodecyl-β-D-maltoside, 1 mM DTT, 1 μM leupeptin, 10 μM NAD and NADP (0.9–1.81 mg/ml)) were assayed by monitoring the production of either [15-^{3}H]retinol (reduction of retinal) or [4-^{3}H]NADPH (oxidation of retinol) (24,28). RDH activities were measured using the phase partition assay (29) or HPLC assays as described (24).

Preparation of RDH5 Affinity Column—Monoclonal anti-RDH5 antibody was purified on a protein-A column, and then the purified antibody was coupled to CNBr-activated Sepharose 4B (Amersham Biosciences) following the manufacturer's procedures.

Purification of RDH5 and RDH5-His_6 from Bovine RPE Microsomes and RDH5-His_6-transfected Sf9 Cells, Respectively—RPE microsomes (1.3 ml, 5 mg/ml) were solubilized with 5 mM *n*-dodecyl-β-D-maltoside in the presence of 20 mM BTP, pH 7.4, 1 mM DTT, and 1 μM leupeptin (buffer A) with 20 μM NAD and NADP for 60 min on ice. The solubilized mixtures were centrifuged at 71,700 × *g* for 40 min, and the supernatant was loaded onto the monoclonal anti-RDH5 antibodies Sepharose 4B (~0.6 ml of gel) equilibrated with buffer A. The column

was then washed with 12 ml of the same buffer, RDH5 was eluted by 45 mM sodium citrate, pH 3.0, 5 mM *n*-dodecyl-β-D-maltoside, and 1 mM DTT, and the fraction was immediately neutralized with 1.35 M Tris-HCl, pH 8.8, to ~pH 6–7. The purification of RDH5-His_6 from the transfected Sf9 cells (~1.5 ml of cell pellets) was carried out similarly except using solubilization buffer at a final volume of 6 ml and 1 ml of gel.

RDH Assays with Sepharose-Antibody-bound RDHs—Sepharose-antibody-bound RDH activities and substrate specificities were carried out by monitoring the production of [15-^{3}H] retinol (reduction of retinal) (24). The reaction mixture (150 μl) contained MES (final concentration, 70–74 mM, pH 5.5), DTT (1 mM), pro-*S* [4-^{3}H]NADH (26 μM), or pro-*S* [4-^{3}H] NADPH (26 μM), 20–25 μl of Sepharose-antibody-bound RDH gel suspension (suspended in 2× volumes of buffer A) in the presence or absence of NAD(P)H (520 μM), and 2 μl of retinal (120–140 μM) substrate stock was added last to initiate the reaction. The reaction was incubated at 37 °C for 50 min then terminated with 400 μl of methanol and 100 μl of 1 M NaCl and extracted with 500 μl of hexane. Radioactivity was measured in the organic phase by scintillation counting.

RESULTS

Initial screening of prostate short chain dehydrogenase/reductase I (PSDR1) expression, an enzyme cloned by Nelson and co-workers (20) from prostate epithelium, reveals that this enzyme is also expressed in the eye (data not shown). Therefore, the name PSDR1 was changed into RDH11 to reflect its broader expression.

RDH11–14 Sequence Analyses and Gene Structures—Nucleic acid and protein sequence databases were searched with the RDH11 cDNA sequence (identical to the sequence of the *PSDR1* gene product (20)) using Blast. This search identified full-length cDNA clones that show homology to RDH11 and encode RDH12 (first deposited by T. Isogai and under accession number AK054835), RDH13 (expressed sequence tag (EST) deposited by R. Strausberg and under accession number BE736147), and RDH14 (also named PAN2 and deposited by Z. Krozowski under accession number AF237952). The analysis of these cDNAs shows open reading frames of 316, 331, and 336 amino acids for RDH12, RDH13, and RDH14, respectively, encoding proteins of ~35, ~36, and ~37 kDa. RDH11 shares 79% similarity with RDH12 and ~60% similarity with RDH13 and RDH14. RDH12, RDH13, and RDH14 share ~60% similarity among themselves (Fig. 1, *A* and *B*).

These proteins contain two motifs highly conserved among SDRs, the cofactor-binding site (G*XXX*G*X*G) and catalytic residues (Y*XXX*K). SDRs contain a motif at the amino terminus consisting of β-strand A, α-helix B, β-strand B, and α-helix C (part of the βA-αB-βB-αC-βC-αD-βD that forms the Rossman fold), which interacts with the adenosine monophosphate moiety of the cofactor. The residues present at the junctions βA-αB and βB-αC are thought to be important in selectivity for NAD(H) *versus* NADP(H). For favorable interaction with NADP(H), positively charged residues are present at the βA-αB junction (glycine-rich motif) and/or at the beginning of α-helix C (7). For all RDH11–14, no charged amino acids are present in the Gly-rich motif (GANTGIG for RDH11–13 or GANSGLG for RDH14), and there are positively charged residues present at the βB-αC junction (**R**DVE**K, R**DVL**K, R**DME**K, R**D**R**A**R**A for RDH11, -12, -13, and -14, respectively), suggesting a preference for NADP/NADPH (Fig. 1A).

The tissue distribution of RDH11–14 was deduced from the array of ESTs displayed in databases corresponding to these RDHs. RDH11 was reported to be expressed abundantly in prostate tissue but also in eye, kidney, pancreas, liver, testis, heart, and brain (20). In addition, ESTs corresponding to RDH11 were also found in libraries from eye, skin, and muscle. ESTs

matching RDH12 were identified in multiple tissues, most of them from eye, but also some from kidney, brain, skeletal muscle, and stomach. RDH13 ESTs were obtained mostly from eye, pancreas, placenta, and lung. Many ESTs from brain, kidney, pancreas, and placenta correspond to RDH14.

Genomic clones were identified by GenBank™ data base searches with the coding sequences of the *RDH*s. Clone Hs14_10185 contains both entire human *RDH11* and *RDH12* genes. The *RDH11* gene is located ~30 kb from the *RDH12* gene in the 3′-*RDH11*-5′ 5′-*RDH12*-3′ orientation. This genomic clone originates from chromosome 14 at q23.3. These genes are located at the locus for a recessive blinding disease, Leber's congenital amaurosis 3 (LCA3) (www.sph.uth.tmc.edu/Retnet). Clone AC011476.7, obtained from chromosome 19 at q13.42, contains the complete *RDH13* gene. Clone Hs2_16082 contains the *RDH14* gene and originates from chromosome 2 at p24.1. Comparison of the *RDH* cDNAs with these genomic clones solved the gene structures. The gene structures of *RDH11*, *RDH12*, and *RDH13* are almost identical and are interrupted by six introns. The intron/exon junctions of *RDH11* and *RDH12* are at the same positions, whereas intron 6 of *RDH13* is positioned 35 amino acids upstream compared with intron 6 of *RDH11* and *RDH12*. *RDH14* has only one intron, which is located at the same position as intron 3 of *RDH11*, *RDH12*, and *RDH13*, and is a relatively small gene (~6 kb compared with 13–18 kb for the *RDH11-13*) (Fig. 1C). This gene structure is different from other SDR superfamily *RDH*s expressed in the eye (30-32).

Localization of RDH11–14 in the Eye—A monoclonal antibody specific for RDH11 did not cross-react with RDH5, a prominent enzyme present in the RPE as shown by immuno-blotting (Fig. 2A). The lack of cross-reactivity is apparent because RDH5 and RDH11 have different molecular masses. Strong immunoreactivity was detected in bovine and monkey RPE (Fig. 2, *C* and *F*) and was blocked by RDH11 peptides (Fig. 2, *D* and *G*). A lower level of RDH11 expression was also detected in the Müller cells, as demonstrated by a double immunolabeling study with the Müller cell marker glial fibrillary acidic protein (Fig. 2H).

A digoxigenin-conjugated RDH12 antisense RNA probe hybridized to the base of monkey photoreceptor inner segments (Fig. 3, *A* and *B*, *left*). To visualize the chromogenic signal in RPE cells, an albino mouse retina was examined in this study (Fig. 3B). In albino mouse (BALB/c) retina (Fig. 3B, *left*), signals were not observed in the RPE cell layer. As a negative control, the sense RDH12 RNA probe did not produce significant hybridization signals in monkey or mouse retina (Fig. 3, *A* and *B*, *right*). No specific anti-RDH12 antibodies have been generated so far.

Antibodies recognizing RDH13 (Fig. 4A) labeled inner segments of the photoreceptor cells of human and monkey retina (Fig. 4, *C* and *F*). Weak signals were observed in a small population of inner nuclear neurons and the inner plexiform layer. Higher magnification images localized RDH13 expression to inner segments of rod and cone photoreceptors (Fig. 4H, *inset*). This immunoreactivity is specific as it was blocked by purified RDH13 protein. RDH14 yielded hybridization signals in the photoreceptor nuclear layer, and this enzyme appears to be expressed at low levels in the eye, although RDH14 immunolabeling was clearly observed in the bovine cone and ROS with a weaker signal in Müller cells (Supplemental Fig. 1).

RDH Activity of RDH11, RDH12, and RDH14—RDH11 catalyzed the reduction of all-*trans*-retinal and its 9-*cis*-, 11-*cis*-, and 13-*cis*-retinal isomers. The activity was observed in the presence of NADPH and with Sf9 insect cell membranes only when Sf9 cells were transfected with the cDNA encoding RDH11 (Fig. 5). The products were clearly identified by the characteristic spectrum for each retinol isomer and a retention time that was similar to authentic standards (Fig. 5). This analysis avoids problems associated with the isomerization among retinols during incubation or sample handling. The activity toward 13-*cis*- was the lowest of

the retinoid substrates tested and was only detected using high sensitivity HPLC analysis. The summary of the product conversion is illustrated in Fig. 6A. RDH12 and RDH14 have very similar properties to those of RDH11 (Fig. 6, *B* and *C*). However, RDH13, expressed in insect cells (Fig. 4), displayed no RDH activity. The double specificity exhibited by RDH11, RDH12, and RDH14 toward *cis*- and all-*trans*-retinoids makes these enzymes unique among short chain RDHs.

RDH11, RDH12, and RDH14 demonstrate a clear specificity for the pro-*S* hydrogen on C4 of NADPH (shown only for one enzyme, Fig. 6D) and the pro-*R* hydrogen on C_{15} of all highly active retinols (Fig. 6E). These properties resemble those of the photoreceptor dehydrogenase, prRDH (24,31), and not those of the RPE enzyme RDH5 (16,24), which is active toward the pro-*S* position of both substrates. The results also suggest that these enzymes catalyze the reaction in both directions, NADPH/retinals ↔ NADP/retinols. RDH11, RDH12, and RDH14 show equal utilization of 11-*cis*-retinal and all-*trans*-retinal when these substrates are present at equal concentrations in the same mixture (data not shown), a property that suggests similar efficiency toward both substrates. No steroid dehydrogenase activity was detected for RDH11, RDH12, and RDH14. The activity of the RDH11–14, photoreceptor prRDH, and RDH5 was potently inhibited by retinoic acids (for example, 9-*cis*-retinoic acid, K_I ~1 μM for RDH11), recombinant CRBP1 (Supplemental Table 1, prRDH), and CRALBP (Supplemental Table 2, RDH5).

Co-purification of RDH5 and RDH11 and Expression of RDHs in Immortal ARPE19 Cells—When RDH5 was purified from RPE membranes using anti-RDH5 monoclonal antibody affinity chromatography, NAD(H)-dependent (RDH5) and NADP(H)-dependent (RDH11) enzymes were also isolated based on immunoblotting and retinol activity profiles (Fig. 7A). The activity was suppressed by diluting [4-^{3}H]NADH with NADH and NADPH. Because the anti-RDH5 antibody did not cross-react with RDH11 (Fig. 2A), these results suggest that both enzymes may form a larger oligomeric structure and/or interact with each other. However, when RDH5 was expressed and purified from insect cells using anti-RDH5 monoclonal antibody affinity chromatography, only NADH- and *cis*-retinoid preferable properties were observed (Fig. 7B). Qualitatively, the stereospecificity of the mixture of RDHs isolated from RPE membranes (Fig. 7A) matched the sum of stereo-preferences toward retinals of RDH5 (Fig. 7B) and RDH11 (Figs. 5 and 6) or the sum of stereo-preferences of RDH5 (Fig. 7B) and the remaining activity in RPE membranes derived from *rdh5*−/− mice (Fig. 7C). This suggests that the enzyme responsible for oxidation of 11-*cis*-retinol in these membranes is RDH11.

As with many enzymes involved in retinoid metabolism, the expression of RDH11 and RDH5 are lost in ARPE19, an immortalized RPE cell line (Supplemental Fig. 2*A*), although other functions of retinal epithelium are preserved. These cells also lack RDH activity toward retinals (Supplemental Fig. 2*B*). These findings are not due to a secondary effect caused by a lack of other retinoid-processing enzymes because transfecting these cells with the RDH11 or 12 cDNAs restores RDH activity. This observation supports the hypothesis that RDH11 is involved in 11-*cis*-retinol oxidation in the RPE (Supplemental Fig. 2*C*).

DISCUSSION

Dual-substrate Specificity, Dual Responsibility; Mechanistic Considerations and Physiological Implications—Studies of stereochemical transformations catalyzed by RDH enzymes in native tissues and in heterologous expression systems provide important insights detailing physiological substrates, cofactors, and potential complementary enzyme activities. Here, we demonstrated that RDH11–14 catalyze hydrogen transfer from the pro-*S* C_4 position of NADPH but not of NADH. This specificity is also observed in the eye, one of the most active tissues in retinoid metabolism (2,24). For all convergently evolved RDH enzymes from

the SDR superfamily, only one conformational orientation of dinucleotides within the binding site has been observed. This is consistent with the structural conservation and rigidity of the Rossman fold (33-37). However, the binding of hydrophobic substrates occurs in less conserved loop regions and can take place by projecting the aldehyde group in *re*- or *si*-face orientation toward the nucleotide (24). It is possible that RDH11–14 will have a mixed stereospecificity for different geometric analogs. For RDH11–14, the binding of dramatically different geometric isomers, such as all-*trans*-, 9-*cis*-, and 11-*cis*-retinoids and poor utilization of 13-*cis*-retinol/al suggest that the enzymes specially recognize the conformation along the C_{12}-C_{15} carbon chain. The observed pro-*R* specificity of RDH12 is identical to the specificity of prRDH, a photoreceptor RDH, and allows its discrimination from other pro-*S*SDRs, including RDH5 (24). However, RDH11–14 differ even from prRDH and other RDHs, which are sensitive for the location of the C_{15} atom and, therefore, recognize *cis* or *trans* isomers. This property also differs from that of two highly homologous tropinone reductases that are members of the SDR superfamily and bind the same substrate differently to produce two different conformations of the product (36). The stereospecific enzymatic properties of RDH11 uniquely match the RDH activity present in RPE membranes of *rdh5*−/− mice (16) and, together with high expression in RPE cells and formation of a complex with RDH5, support the idea that RDH11 is the missing enzyme of the visual cycle responsible for production of 11-*cis*- and all-*trans*-retinal. These studies also provide a novel approach for the analysis of complex and redundant enzymatic pathways and for the in-depth use of stereochemistry in studies of metabolic transformations.

Retinoid Flow in the Eye—RDH11 localizes in RPE, where it likely plays a key role in producing the aldehyde forms of all-*trans* and 11-*cis* isomers (Fig. 8). All-*trans*-retinal is utilized by retinal G-protein-coupled receptor, a hypothetical photoisomerase that is essential for replenishing 11-*cis*-retinals at high illumination levels (38). It has been proposed that RDH5 forms a complex with this retinal G-protein-coupled receptor (39). Here, we showed that RDH11 may interact with RDH5 (Fig. 7A), forming possible homo- and heterodimeric or oligomeric complexes (7).

Another function of RDH11, along with RDH5, might be to produce 11-*cis*-retinal from 11-*cis*-retinol. RDH5 is responsible for the majority of RDH activity in RPE membranes. In humans, mutations in this gene are associated with fundus albipunctatus, a disease expressed by delayed dark adaptation of both cones and rods. Detailed analyses of *rdh5*−/− mice have identified only a minor phenotype manifested by the accumulation of 13-*cis*-retinoids. These studies indicate that another enzyme is responsible for the production of 11-*cis*-retinal under bleaching conditions (16). The RDH(s) responsible for the production of 11-*cis*-retinal in RPE membrane from *rdh5*−/− mice display pro-*S* hydrogen specificity for NADPH and utilize 9-*cis*- and 11-*cis*-retinal but not 13-*cis*-retinal (16). Furthermore, pro-*R* stereospecificity toward 11-*cis*-retinol with NADP was observed in bovine RPE (24). The pro-*R* stereospecificity toward the retinols is a rare property among SDRs. These results are in perfect agreement with the properties of RDH11 determined in the experiments reported here (Figs. 5-7). Therefore, it is highly probable that RDH11 is the missing enzyme of the RPE in vertebrates as no other known RDH exhibits similar properties (Supplemental Table 3).

RDH12 is expressed in photoreceptor cells, although RDH14 appears to be a minor enzymatic component of ocular retinoid metabolism based upon its level of expression. The substrate specificity of RDH12 indicates that it functions in a fashion complementary to previously identified RDHs (31,32) involved in the production of all-*trans*-retinol from all-*trans*-retinal. We hypothesize that RDH12 might be the key enzyme in the formation of 11-*cis*-retinal from 11-*cis*-retinol during regeneration of the cone visual pigments (for review, see Ref. 2).

Bliss reports that the equilibrium constant for reduction of all-*trans*-retinal is 10^{-2} to 10 between pH 6.6 to 9.4, respectively (40). Depending on the layer of the retina, the ratio of NADP to NADPH is between 4 to 1 and 1.5 to 1, whereas the ratio of NAD to NADH could be as high as 300 to 1 (41). Therefore, NAD-dependent enzymes will be mostly oxidizing RDHs, whereas NADP-dependent enzymes will have the ability to catalyze reactions in both directions depending on the retinol/retinal ratio.

Involvement of RDH11–14 in Retinoid Transformation and All-trans- and 9-cis-Retinoic Acid Production—The *RDH5* gene product has been implicated in the production of 9-*cis*-retinal before this aldehyde is further oxidized to 9-*cis*-retinoic acids (12,14). However, disabling mutations in men and mice produce no embryonic developmental abnormalities (16-19). In this report, we provide unequivocal evidence that RDH11–14 display high activity toward 9-*cis*- and all-*trans*-retinol. The unique substrate utilization of all-*trans*- and *cis*-retinoids combined with the specific expression of these enzymes identifies a novel pathway involving the cooperative production of both retinoic acids by the same enzyme that may activate combinations of the retinoic acid receptor and retinoid X receptor nuclear receptors (4). In addition, RDH11–14 may participate in the reduction of all-*trans*-retinal and 9-*cis*-retinal because they are formed in reactions catalyzed by dioxygenases from dietary 9-*cis*-β-carotene (42). These retinols are stored in the form of retinyl esters before use. Because 9-*cis*-retinal is more stable than 9-*cis*-retinol, an alternative pathway in the production of 9-*cis*-isomers is the isomerization of all-*trans*-retinol to 9-*cis*-retinol (43). Although the equilibrium is shifted toward the all-*trans*-isomers (5), small amounts of 9-*cis*-retinal would be trapped as it is formed and further oxidized by aldehyde dehydrogenases (44). These RDH properties do not eliminate the possibility that these dehydrogenases may also be involved in redox reactions of other unidentified lipophilic substrates, as has been documented for other SDRs that are fairly unrestricted in substrate recognition (9). SDRs are a redundant group of enzymes regulated by the availability of hydrophobic substrates and the redox potential of the subcellular compartments. However, the localization of the RDH11–14 to cellular and subcellular ocular compartments, where the traffic of retinoids is high, supports the idea that these enzymes are involved in critical retinoid transformations that mediate vision. Targeted genetic lesions that abolish individual or combinations of dual-specificity SDR activities may serve to further determine their specific roles in ocular and developmental processes.

Acknowledgments

We thank Dr. Bryan S. Sires for assistance with preparing human eye tissue from a donor. Legal requirements for use of human donor retinas and primate retinas were met (University of Washington Human Subjects, approval on file).

REFERENCES

1. Polans A, Baehr W, Palczewski K. Trends Neurosci 1996;19:547–554. [PubMed: 8961484]
2. McBee JK, Palczewski K, Baehr W, Pepperberg DR. Prog. Retin. Eye Res 2001;20:469–529. [PubMed: 11390257]
3. Leid M, Kastner P, Chambon P. Trends Biochem. Sci 1992;17:427–433. [PubMed: 1333659]
4. Mangelsdorf DJ, Thummel C, Beato M, Herrlich P, Schutz G, Umesono K, Blumberg B, Kastner P, Mark M, Chambon P. Cell 1995;83:835–839. [PubMed: 8521507]
5. McBee JK, Van Hooser JP, Jang GF, Palczewski K. J. Biol. Chem 2001;276:48483–48493. [PubMed: 11604395]
6. Napoli JL. Biochim. Biophys. Acta 1999;1440:139–162. [PubMed: 10521699]
7. Jornvall H, Persson B, Krook M, Atrian S, Gonzalez-Duarte R, Jeffery J, Ghosh D. Biochemistry 1995;34:6003–6013. [PubMed: 7742302]
8. Chou CF, Lai CL, Chang YC, Duester G, Yin SJ. J. Biol. Chem 2002;277:25209–25216. [PubMed: 11997393]
9. Biswas MG, Russell DW. J. Biol. Chem 1997;272:15959–15966. [PubMed: 9188497]

10. Driessen CA, Janssen BP, Winkens HJ, van Vugt AH, de Leeuw TL, Janssen JJ. Investig. Ophthalmol. Vis. Sci 1995;36:1988–1996. [PubMed: 7544779]
11. Simon A, Hellman U, Wernstedt C, Eriksson U. J. Biol. Chem 1995;270:1107–1112. [PubMed: 7836368]
12. Paik J, Vogel S, Piantedosi R, Sykes A, Blaner WS, Swisshelm K. Biochemistry 2000;39:8073–8084. [PubMed: 10891090]
13. Mertz JR, Shang E, Piantedosi R, Wei S, Wolgemuth DJ, Blaner WS. J. Biol. Chem 1997;272:11744–11749. [PubMed: 9115228]
14. Romert A, Tuvendal P, Simon A, Dencker L, Eriksson U. Proc. Natl. Acad. Sci. U. S. A 1998;95:4404–4409. [PubMed: 9539749]
15. Driessen CA, Winkens HJ, Kuhlmann ED, Janssen AP, van Vugt AH, Deutman AF, Janssen JJ. FEBS Lett 1998;428:135–140. [PubMed: 9654122]
16. Jang GF, Van Hooser JP, Kuksa V, McBee JK, He YG, Janssen JJ, Driessen CA, Palczewski K. J. Biol. Chem 2001;276:32456–32465. [PubMed: 11418621]
17. Driessen CA, Winkens HJ, Hoffmann K, Kuhlmann LD, Janssen BP, Van Vugt AH, Van Hooser JP, Wieringa BE, Deutman AF, Palczewski K, Ruether K, Janssen JJ. Mol. Cell. Biol 2000;20:4275–4287. [PubMed: 10825191]
18. Yamamoto H, Simon A, Eriksson U, Harris E, Berson EL, Dryja TP. Nat. Genet 1999;22:188–191. [PubMed: 10369264]
19. Cideciyan AV, Haeseleer F, Fariss RN, Aleman TS, Jang GF, Verlinde CL, Marmor MF, Jacobson SG, Palczewski K. Visual Neurosci 2000;17:667–678.
20. Lin B, White JT, Ferguson C, Wang S, Vessella R, Bumgarner R, True LD, Hood L, Nelson PS. Cancer Res 2001;61:1611–1618. [PubMed: 11245473]
21. Kedishvili NY, Chumakova OV, Chetyrkin SV, Belyaeva OV, Lapshina EA, Lin DW, Matsumura M, Nelson PS. J. Biol. Chem 2002;277:28909–28915. [PubMed: 12036956]
22. Haeseleer F, Imanishi Y, Saperstein DA, Palczewski K. Investig. Ophthalmol. Vis. Sci 2001;42:3294–3300. [PubMed: 11726636]
23. Imanishi Y, Li N, Sokal I, Sowa ME, Lichtarge O, Wensel TG, Saperstein DA, Baehr W, Palczewski K. Eur. J. Neurosci 2002;15:63–78. [PubMed: 11860507]
24. Jang GF, McBee JK, Alekseev AM, Haeseleer F, Palczewski K. J. Biol. Chem 2000;275:28128–28138. [PubMed: 10871622]
25. Papermaster DS. Methods Enzymol 1982;81:48–52. [PubMed: 6212746]
26. Stecher H, Gelb MH, Saari JC, Palczewski K. J. Biol. Chem 1999;274:8577–8585. [PubMed: 10085092]
27. Mercer, EI.; Scott, TA. Concise Encyclopedia of Biochemistry and Molecular Biology. Walter de Gruyter & Co.; Berlin: 1997.
28. Palczewski K, Jager S, Buczylko J, Crouch RK, Bredberg DL, Hofmann KP, Asson-Batres MA, Saari JC. Biochemistry 1994;33:13741–13750. [PubMed: 7947785]
29. Saari JC, Garwin GG, Haeseleer F, Jang GF, Palczewski K. Methods Enzymol 2000;316:359–371. [PubMed: 10800687]
30. Romert A, Tuvendal P, Tryggvason K, Dencker L, Eriksson U. Exp. Cell Res 2000;256:338–345. [PubMed: 10739682]
31. Rattner A, Smallwood PM, Nathans J. J. Biol. Chem 2000;275:11034–11043. [PubMed: 10753906]
32. Haeseleer F, Palczewski K. Methods Enzymol 2000;316:372–383. [PubMed: 10800688]
33. Ghosh D, Wawrzak Z, Weeks CM, Duax WL, Erman M. Structure (Lond.) 1994;2:629–640.
34. Bennett MJ, Schlegel BP, Jez JM, Penning TM, Lewis M. Biochemistry 1996;35:10702–10711. [PubMed: 8718859]
35. Tanaka N, Nonaka T, Tanabe T, Yoshimoto T, Tsuru D, Mitsui Y. Biochemistry 1996;35:7715–7730. [PubMed: 8672472]
36. Nakajima K, Yamashita A, Akama H, Nakatsu T, Kato H, Hashimoto T, Oda J, Yamada Y. Proc. Natl. Acad. Sci. U. S. A 1998;95:4876–4881. [PubMed: 9560196]

37. Grimm C, Maser E, Mobus E, Klebe G, Reuter K, Ficner R. J. Biol. Chem 2000;275:41333–41339. [PubMed: 11007791]
38. Chen P, Hao W, Rife L, Wang XP, Shen D, Chen J, Ogden T, Van Boemel GB, Wu L, Yang M, Fong HK. Nat. Genet 2001;28:256–260. [PubMed: 11431696]
39. Chen P, Lee TD, Fong HK. J. Biol. Chem 2001;276:21098–21104. [PubMed: 11274198]
40. Bliss AF. Arch. Biochem. Biophys 1951;31:197–204.
41. Matschinsky FM. J. Neurochem 1968;15:643–657. [PubMed: 4386358]
42. Nagao A, Olson JA. FASEB J 1994;8:968–973. [PubMed: 8088462]
43. Van Hooser JP, Aleman TS, He YG, Cideciyan AV, Kuksa V, Pittler SJ, Stone EM, Jacobson SG, Palczewski K. Proc. Natl. Acad. Sci. U. S. A 2000;97:8623–8628. [PubMed: 10869443]
44. Napoli JL. FASEB J 1996;10:993–1001. [PubMed: 8801182]

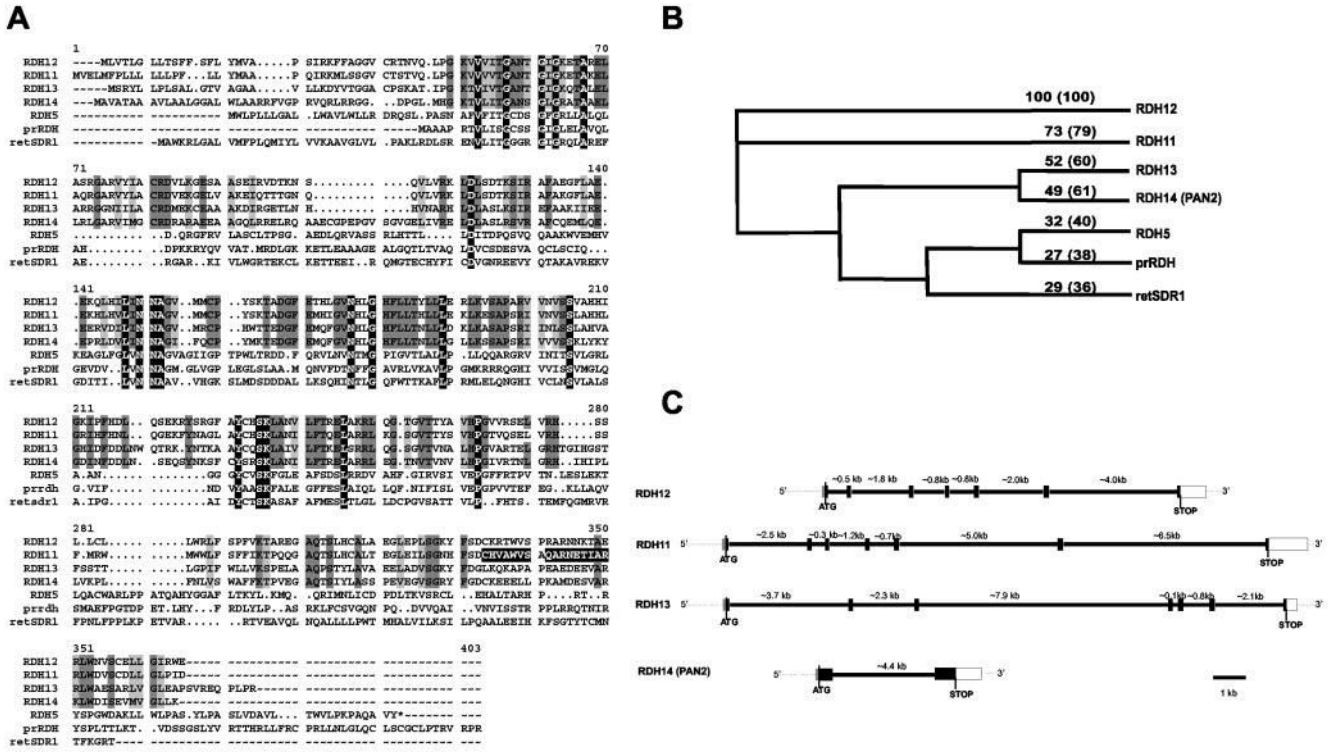

Fig. 1.

Primary sequences and the gene structures of RDHs expressed in the retina. *A*, alignment of the deduced amino acid sequences of human RDH11 (AF167438), human RDH12 (sequence identical to unnamed XM_085058), human RDH13 (sequence identical to unknown AAH09881), human PAN2 (RDH14) (NM_020905), human RDH5 (HSU43559), human prRDH (NM_015725), and human retSDR1 (AF061741). The identical residues in all sequences are shown in *white letters* on a *black background*. The identical residues in RDH11–14 sequences are shown in *dark gray*. The conserved residues in RDH11–14 sequences are shown in *light gray*. The amino acids used to develop anti-RDH11 monoclonal antibodies are indicated by *white letters* on the *black background*. *B*, phylogenetic tree. The tree was built with a bootstrap analysis of neighbor-joining distance using PAUPSearch in GCG (Genetics Computer Group). The *numbers* represent the percentage of identities with RDH12. The percentage of similarities is indicated in parentheses. *C*, gene structure of RDH11–14. The coding regions are shown as *black boxes*, and the noncoding regions are shown as *white boxes*. The *thick lines* and the *numbers* represent the introns and their sizes, respectively.

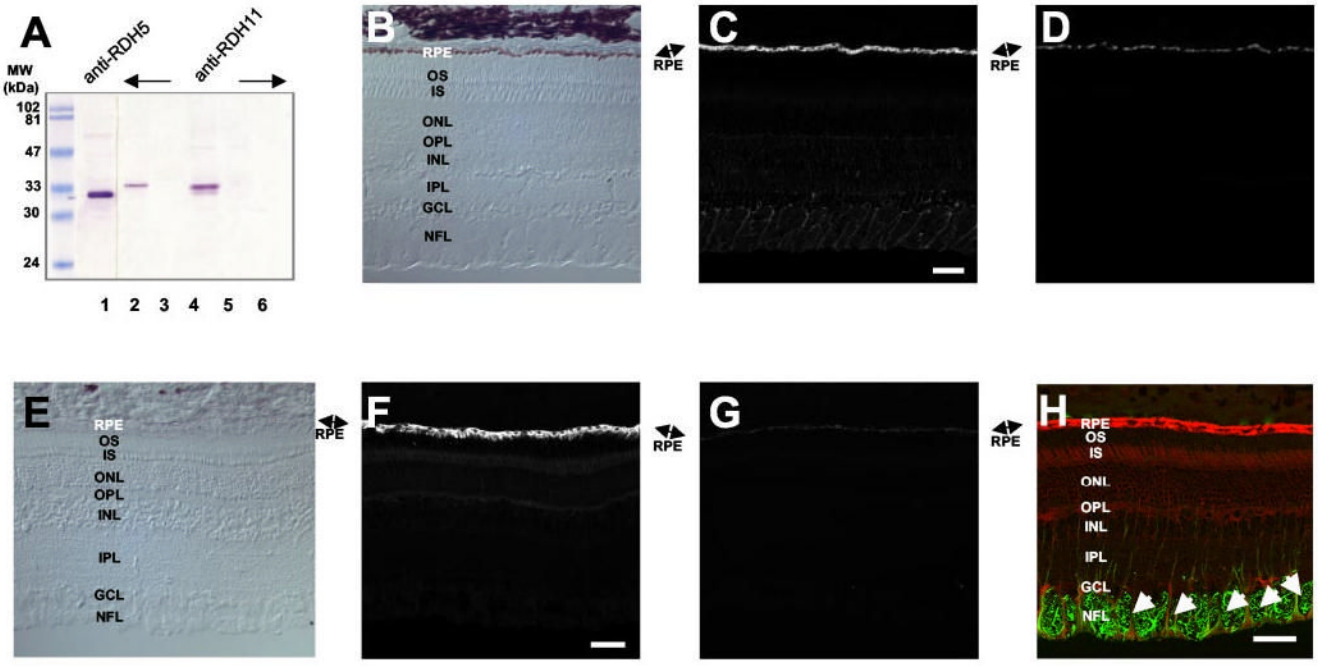

Fig. 2.

Immunolocalization of RDH11 in bovine and monkey retina. *A*, specificity of anti-RDH5 (*lane 1*) and anti-RDH11 (*lanes 2–5*) antibodies. *Lanes 1* and *2*, bovine RPE; *lane 3*, bovine ROS; *lane 4*, Sf9 cell lysate expressing recombinant RDH11; *lane 5*, Sf9 cell lysate; *lane 6*, purified RDH5-His_6. *B–D*, immunofluorescence localization of RDH11 in monkey retina. *B*, control bright field image of monkey retina. *C*, RDH11 immunolabeling is predominant in the RPE cell layer of monkey retina. *D*, addition of purified peptide (0.5 μg/ml) abolishes RDH11 immunoreactivity. *E–G*, immunofluorescence localization of RDH11 in bovine retina. *E*, control bright field image of bovine retina. *F*, RDH11 immunolabeling is predominant in the RPE cell layer of bovine retina. *G*, addition of purified peptide (0.5 μg/ml) abolishes RDH11 immunoreactivity. *Bar*, 50 μm. *H*, co-localization of RDH11 and glial fibrillary acidic protein in the inner retina. The bovine retina section was double-labeled with antibodies to glial fibrillary acidic protein and RDH11. *Arrows* show the colocalization of glial fibrillary acidic protein (*green*) and RDH11 (*red*) in Müller cells. *Bar*,50 μm. *OS*, photoreceptor outer segments; *IS*, photoreceptor inner segments; *ONL*, outer nuclear layer; *OPL*, outer plexiform layer; *INL*, inner nuclear layer; *IPL*, inner plexiform layer; *GCL*, ganglion cell layer; *NFL*, nerve-fiber layer.

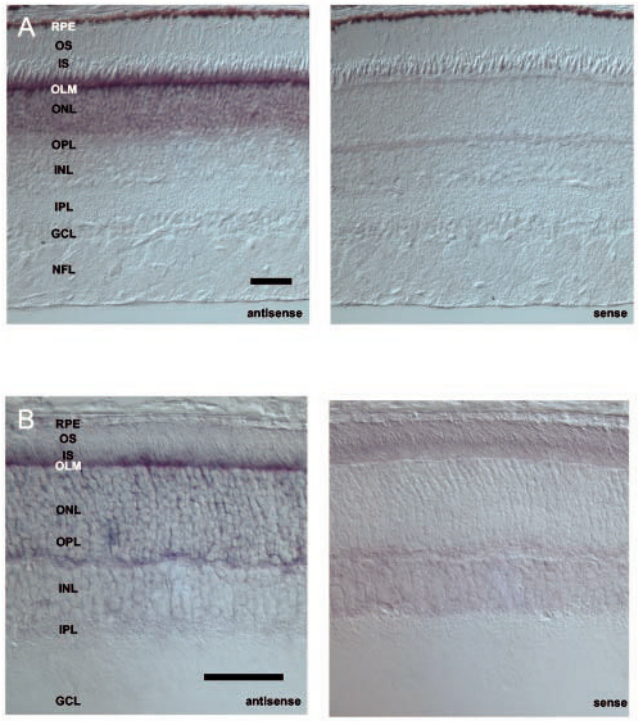

Fig. 3.

***In situ* hybridization of monkey and mouse RDH12.** *A*, *in situ* hybridization of RDH12 transcripts in monkey retina using antisense (*left*) and sense (*right*) RNA. The strongest signal is detected in photoreceptor (cones and rods) inner segments and cell bodies. *B*, *in situ* hybridization of RDH12 transcripts in mouse retina using antisense (*left*) and sense (*right*) RNA. The strongest signal is detected in photo-receptor inner segments. *Bar*, 50 μm. *RPE*, retinal pigment epithelium; *OS*, photoreceptor outer segments; *IS*, photoreceptor inner segments; *OLM*, outer limiting membrane; *ONL*, outer nuclear layer; *OPL*, outer plexiform layer; *INL*, inner nuclear layer; *IPL*, inner plexiform layer; *GCL*, ganglion cell layer; *NFL*, nerve-fiber layer.

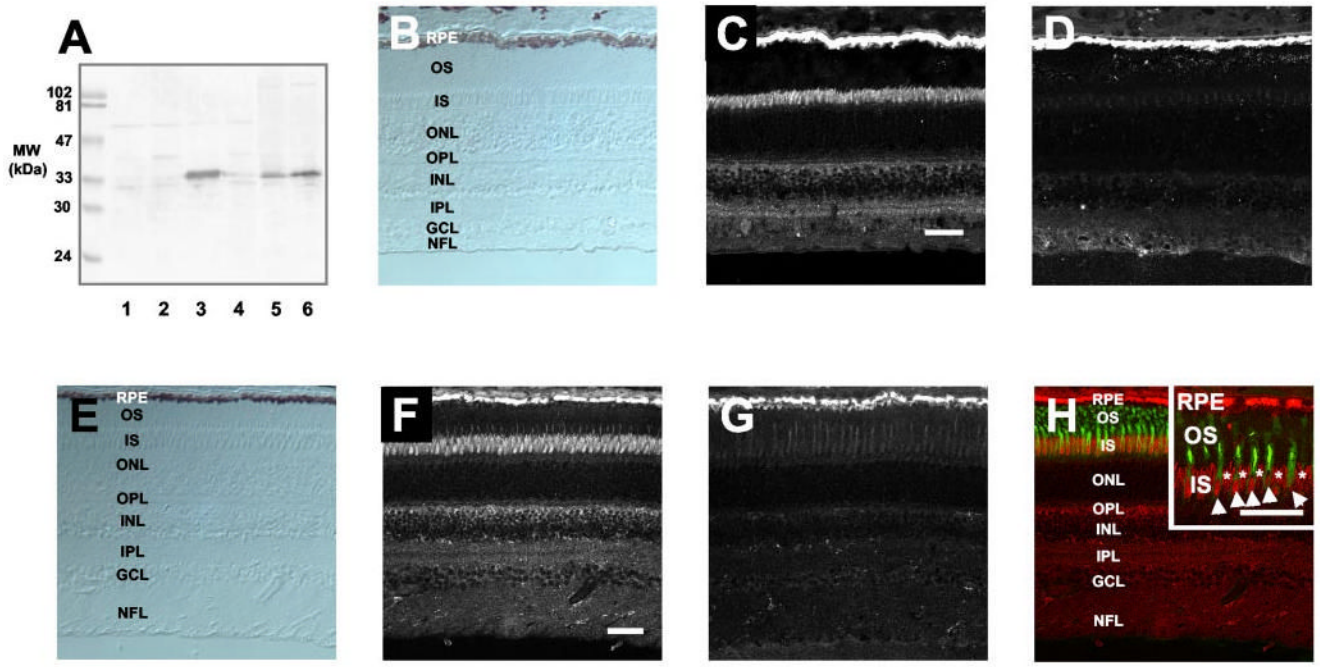

Fig. 4.

Immunolocalization of RDH13 in human and monkey retina. *A*, specificity of anti-RDH13 antibodies. *Lane 1*, SF9 cell lysate expressing recombinant RDH11; *lane 2*, SF9 cell lysate expressing recombinant RDH12; *lane 3*, SF9 cell lysate expressing recombinant RDH13; *lane 4*, SF9 cell lysate expressing recombinant RDH14; *lane 5*, monkey retinal homogenate; *lane 6*, human retinal homogenate. *B–D*, immunofluorescence localization of RDH13 in human retina. *B*, bright field image of human retina. *C*, RDH13 immunolabeling is predominant in the photoreceptor inner segments of human retina. Weak signals were observed in the inner plexiform layer and inner nuclear neurons proximal to the outer plexiform layer. *D*, addition of purified RDH13 (2 μg/ml) abolishes RDH13 immunoreactivity. *E–G*, immunofluorescence localization of RDH13 in monkey retina. *E*, bright field image of monkey retina. *F*, RDH13 immunolabeling is predominant in the photoreceptor inner segments of monkey retina. Weak signals were observed in inner plexiform layer and inner nuclear neurons proximal to the outer plexiform layer. *Bar*, 50 μm. *G*, addition of purified RDH13 (2 μg/ml) abolishes RDH13 immunoreactivity. *H*, localization of RDH13 (*red*) in monkey retina. The cone sheath was simultaneously visualized by fluorescein-conjugated peanut agglutinin (*green*). *Inset*, higher magnification image. *Arrows* show the localization of RDH13 (*red*) in cone inner segments surrounded by the cone sheath (*green*). *Asterisks* indicate the localization of RDH13 in rod inner segments. *Bar*, 50 μm. *RPE*, retinal pigment epithelium; *OS*, photoreceptor outer segments; *IS*, photoreceptor inner segments; *ONL*, outer nuclear layer; *OPL*, outer plexiform layer; *INL*, inner nuclear layer; *IPL*, inner plexiform layer; *GCL*, ganglion cell layer; *NFL*, nerve-fiber layer.

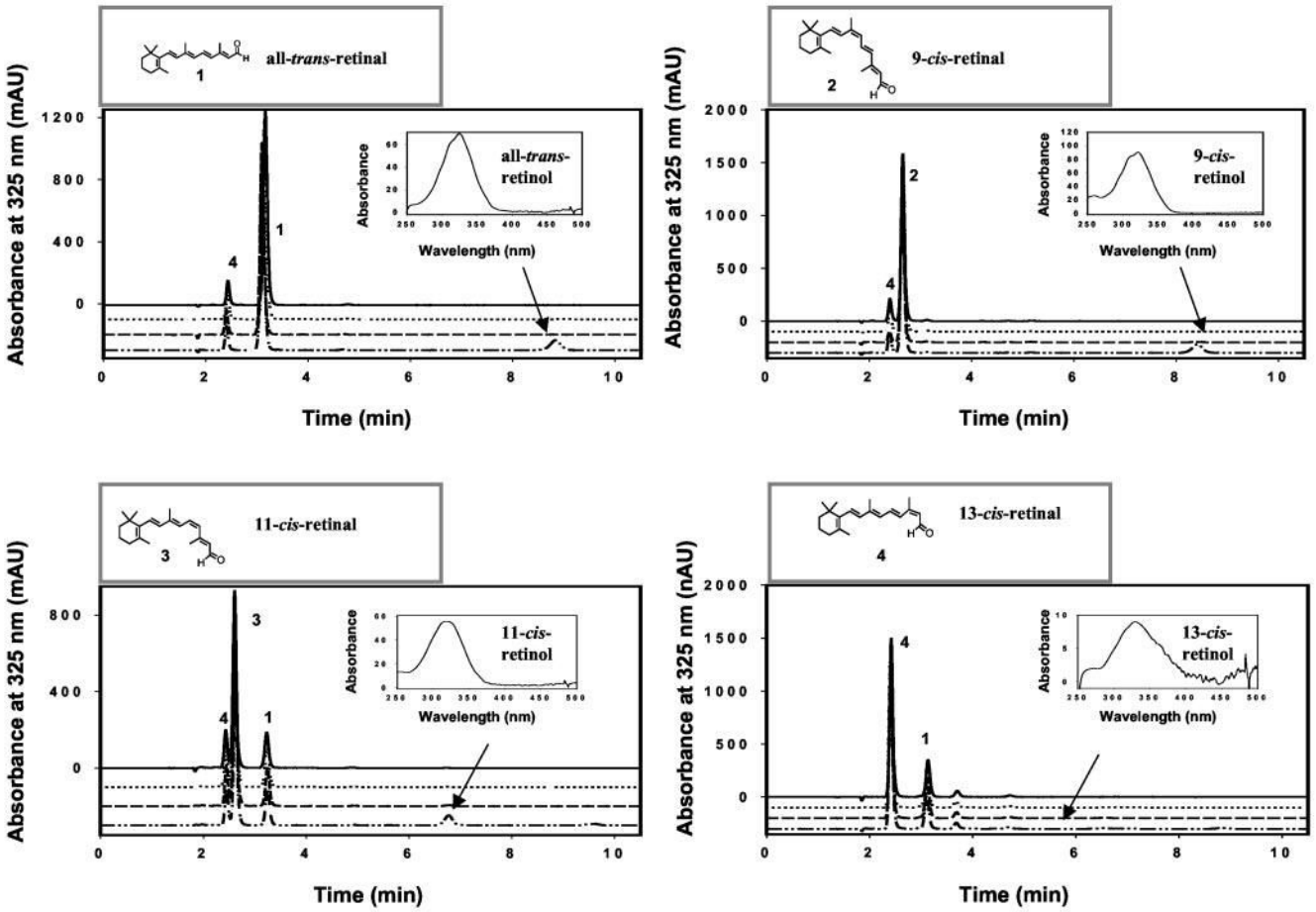

Fig. 5.

RDH activity with various isomers of retinals and NADH and NADPH dinucleotides. In each panel, the *first* (from the top) and *third* chromatograms were from bacmid in Sf9 cells with NADH (*solid lines*) and NADPH (*dashed lines*) as dinucleotide substrates, respectively. The second and fourth chromatograms were from recombinant RDH11 expressed in Sf9 cells using NADH (*dotted lines*) and NADPH (*dashed-dotted lines*) as dinucleotide substrates, respectively. Retinols (indicated by *arrows* identifying specific elution times and spectra (*insets*)) were only produced when RDH11 expressed in Sf9 cells and NADPH were used. The assays (reduction of retinals) were carried out using non-radiolabeled retinals (90 μM) and dinucleotides (50 μM), as described under "Materials and Methods." The retinoids were separated using a normal phase HPLC column (Beckman, Ultrasphere-Si, 2.1 mm × 250 mm) developed with 10% ethyl acetate, 90% hexane at a flow rate of 0.5 ml/min. Note that the spontaneous isomerization of retinal generated a mixture of aldehydes, for example all-*trans*-retinal (1) is contaminated by 13-*cis*-retinal (4), and the production of 13-*cis*-retinol is at the level of background (*fourth panel*). *mAU*, milliabsorbance units.

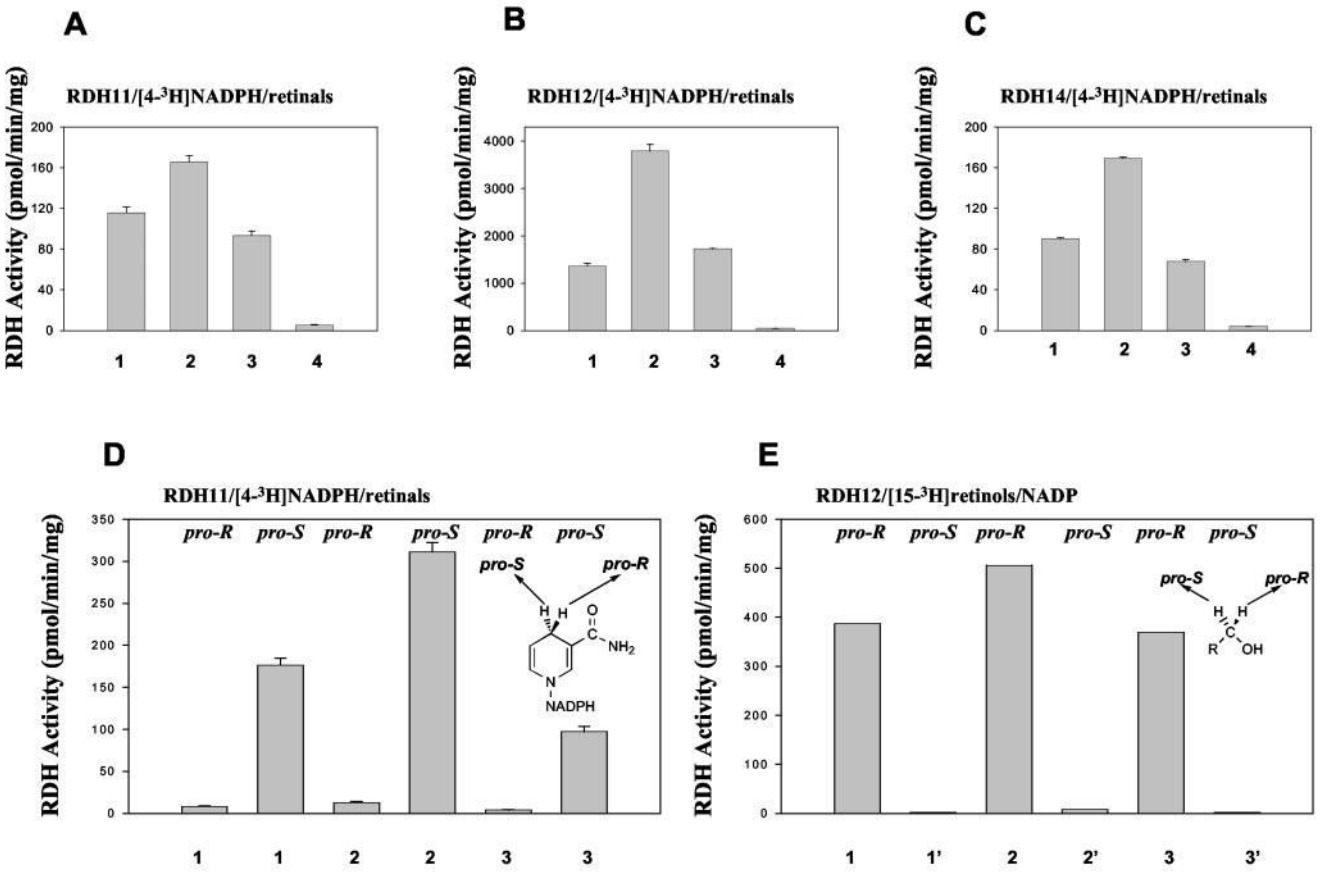

Fig. 6.

Stereoisomeric specificities of RDH11–14. *A–C*, different geometric isomers of retinals (*1*, all-*trans*-retinal; *2*, 9-*cis*-retinal; *3*, 11-*cis*-retinal; *4*, 13-*cis*-retinal, 90 μM each) were tested with various RDHs in the presence of stereospecifically radiolabeled pro-*S* [4-^{3}H]NADPH (18 μM). The assay (reduction of retinals) and HPLC conditions were the same as in Fig. 5. The corresponding retinol fraction was collected and subjected to scintillation counting. *D*, stereospecifically radiolabeled pro-*R* [4-^{3}H]NADPH (20 μM) or pro-*S* [4-^{3}H]NADPH (18 μM) was tested with RDH11 using various retinals (1-3). The partition assay for retinal reduction was used to measure the activity, as described under "Materials and Methods." *E*, stereospecifically labeled pro-*R* [15-^{3}H]retinols (*1′*, all-*trans*-retinol; *2′*, 9-*cis*-retinol; *3′*, 11-*cis*-retinol, 40–60 μM) or pro-*S* [15-^{3}H]retinols (40–60 μM) were examined with RDH12 in the presence of NADP (700 μM) at pH 8.0. The partition assay for retinol oxidation was used to measure the activity as described under "Materials and Methods."

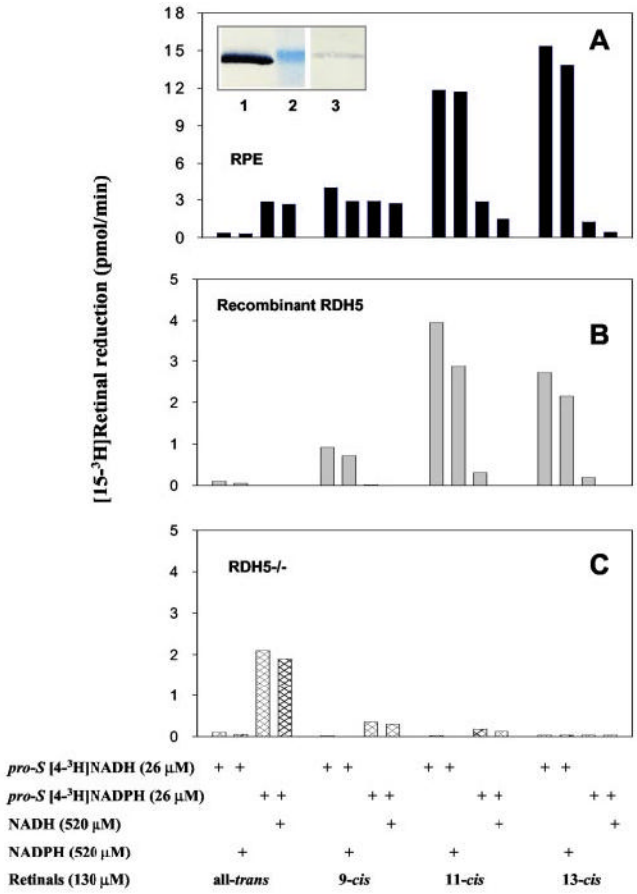

Fig. 7.

Enzymatic activities and RDH11 immunoreactivity of affinity column-purified of RDH5. *A*, RDH5 from bovine RPE microsomes was purified as described under "Materials and Methods." The assay with pro-*S* [4-^{3}H]NAD(P)H and geometric isomers of retinals in the presence or absence of NAD(P)H was carried out for 50 min at 37 °C using the phase partition assay as described under "Materials and Methods," and the amount of [15-^{3}H]retinol isomer was quantified. *B*, RDH5-His$_6$ from transfected Sf9 cells was purified as described under "Materials and Methods." The assay was carried out for 50 min at 37 °C using phase partition assay as described under "Materials and Methods." Indicated is the amount of the corresponding [15-^{3}H]retinol isomer formed in pmol/min. *Inset*, immunoblot of the purified fraction on anti-RDH5 antibody column probed with specific anti-RDH5 (*lane 1*) and RDH11 antibodies (*lane 3*). *Lane 2* is a 33-kDa molecular marker. *C*, stereospecificity toward retinal in RPE membranes derived from *rdh5*−/− mice (16).

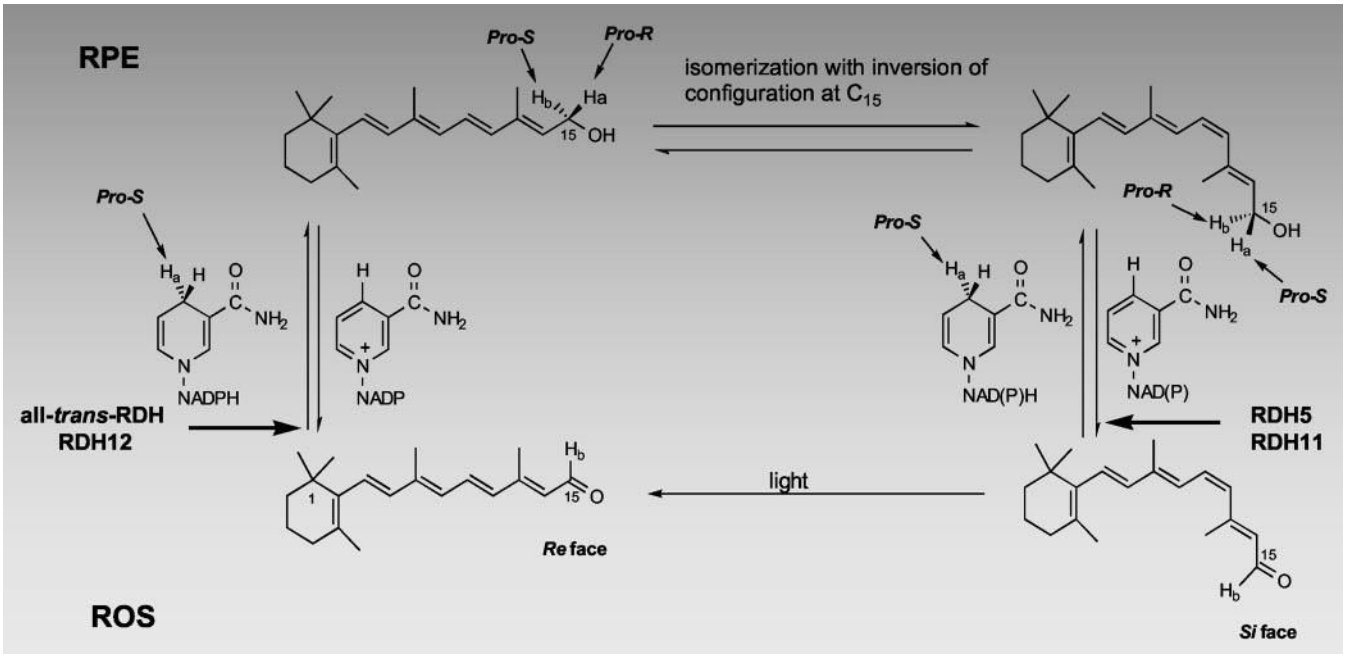

Fig. 8.

Isomeric specificity of the retinoid cycle reactions in the vertebrate retina. Light causes the isomerization of rhodopsin chromophore, 11-*cis*-retinal, to all-*trans*-retinal, which is next reduced in the reaction catalyzed by all-*trans*-retinal-specific RDH(s). This dehydrogenase activity utilizes pro-*S* [4-H_a] of NADPH and does not bind NADH to generate pro-*R* [15-H_a] all-*trans*-retinol. Next, pro-*R* [15-H_a]all-*trans*-retinol or its derivative is isomerized with the inversion of the C_{15} prochiral methylene hydroxyl group configuration, specifically generating pro-*S* [15-H_a]11-*cis*-retinol isomer. Pro-*S* [15-H_a]11-*cis*-retinol isomer is then oxidized by RDH5 activity (resulting in the loss of pro-*S* [15-H_a]) or by RDH11 (resulting in the loss of pro-*R* [15-H_b]) to 11-*cis*-retinal with concomitant generation of pro-*S* [4-H_a]NADH or pro-*S* [4-H_b]NADPH to complete the cycle (modified version from (24)).

Table I

Syntheses of various stereospecific 15-^{3}H-labeled retinols by dehydrogenases

Retinols[a]	Reaction mixture[b]
All-*trans*-retinol	
Pro-*R* all-*trans*-[15-^{3}H]retinol	ROS (1 mg of rhodopsin in 500 μl of 20 mM BTP, pH 7.4, 0.1 M NaCl), DTT, [^{3}H]NADPH[c] (141 nmol), and all-*trans*-retinal (562.5 nmol) in 3.5 ml of 65 mM MES, pH 5.5.
Pro-*S* all-*trans*-[15-^{3}H]retinol	ROS (1 mg of rhodopsin in 500 μl of 20 mM BTP, pH 7.4, 0.1 M NaCl), DTT, all-*trans*-[15-^{3}H]retinal (242 nmol), NADPH (7.26 μmol) in 3.5 ml of 78 mM MES, pH 5.5.
9-*cis*-Retinol	
Pro-*R* 9-*cis*-[15-^{3}H]retinol	Horse liver alcohol dehydrogenase (0.3 mg), NADH (7.6 μmol), Tween 80, 9-*cis*-[15-^{3}H]retinol, and DTT in 3.5 ml of 76 mM MES, pH 5.5.
Pro-*S* 9-*cis*-[15-^{3}H]retinol	Horse liver alcohol dehydrogenase (0.3 mg). [^{3}H]NADH (245 nmol), Tween 80, and 9-*cis*-retinal (425 nmol) in 3.2 ml of 60 mM MES, pH 5.5.
11-*cis*-Retinol	
Pro-*R* 11-*cis*-[15-^{3}H]retinol	RDH5[d] (500 μl), DTT, NADH (6.25 μmol), and 11-*cis*-[15-^{3}H]retinol (500 nmol) in 3 ml of 81 mM MES, pH 5.5.
Pro-*S* 11-*cis*-[15-^{3}H]retinol	RDH5[d] (500 μl), DTT, [^{3}H]NADH (291 nmol), and 11-*cis*-retinal (500 nmol) in 4 m of 67.5 mM MES, pH 5.5.

[a] Retinols were extracted with hexane and purified by normal phase HPLC (“Materials and Methods”).

[b] DTT and Tween 80 were 1 mM and 0.025%, respectively. The reaction was incubated at 37 °C for 70 min.

[c] Prepared by [^{3}H]$NaBH_4$ reduction (“Materials and Methods”).

[d] Cells of Sf9-expressed RDH5 suspended (1:50) in 20 mM BTP, pH 7.4, 0.25 mM *n*-dodecyl-β-D-maltoside, 10 μM NAD and NADP, 1 μM DTT, and 1 μM leupeptin.